2013 IEEE International Conference on Robotics and Automation (ICRA)
Karlsruhe, Germany, May 6-10, 2013

Robust Tracking of Bio-Inspired References for a Biped Robot Using Geometric Algebra and Sliding Modes

J. Oviedo-Barriga[1], O. Carbajal-Espinosa[2], L. González-Jiménez[3], B. Castillo-Toledo[4], *Senior Member, IEEE,* and E. Bayro-Corrochano[5], *Senior Member, IEEE*

***Abstract*— Controlling walking biped robots is a challenging problem due to its complex and uncertain dynamics. In order to tackle this, we propose a sliding mode controller based on a dynamic model which was obtained using the conformal geometric algebra approach (CGA). The CGA framework permits us to use lines, points, and other geometric entities, to obtain the Lagrange equations of the system. The references for the joints of the robot were bio-inspired in the kinematics of a walking human body. The first and second derivatives of the reference signal were obtained through an exact robust differentiator based on high order sliding modes. The performance of the proposed control scheme is illustrated through simulation.**

I. INTRODUCTION

The control of bipedal walking robot is a complex task due to several degrees of freedom, highly nonlinear dynamics, and a complicated model to describe the behavior of the walking robot. For this reason, we analyze each leg of the biped robot as a serial robotic system and synthesize the dynamic model via the Lagrange equations using the conformal geometric (CGA) approach. The CGA approach allows us to obtain, through a simple procedure, a compact representation of the dynamics of a robotic mechanism. This is due to the simple representation of rigid transformations (rotations, translations, screw motions and others) and geometric entities (points, lines, planes, circles, spheres, point pairs, etc) in this framework [1].

The references for each joint of the biped robot were obtained using the Humanoid Robots Simulation Platform (HRSP) [2], a *Simulink Toolbox* developed by the group of Aleksandar Rodic [3].

Then, a sliding mode controller was designed to perform tracking of the bio-inspired references for the biped robot. Sliding mode control is widely used in uncertain or disturbed systems, featuring robustness and accuracy [4]. An important drawback of the standard sliding mode controller is the presence of high frequency components in the control signals due to the switching function used in its design. In order to attenuate this effect we use sigmoid functions in the proposed controller.

The authors are with the CINVESTAV, Department of Electrical Engineering and Computer Sciences, Unidad Guadalajara, Zapopan, Jalisco, 45015 México.
(e-mail: joviedo[1], ocarbajal[2], lgonzale[3], toledo[4], edb[5]@ gdl.cinvestav.mx).

The document is organized as follows. Section II presents an introduction to the Conformal Geometric Algebra. The dynamic model for the pose of robotic manipulators is obtained in Section III. The design of the error variables and sliding mode controller in CGA are defined in Section IV. Also, the structure for the exact robust differentiator is presented. Section V shows the application of the designed controllers in a 12 DOF biped robot, via simulation. Finally, some conclusions are given in Section VI.

II. CONFORMAL GEOMETRIC ALGEBRA

The Euclidean vector space $\mathbb{R}^3$ can be represented in geometric algebra $G_{4,1}$ and treat conformal geometry in an advantageous manner [7]. This algebra has an orthonormal vector basis given by $\{e_i\}$ and a bivectorial basis defined as $e_{ij} = e_i \wedge e_j$, for $i, j = \{0,1,2,3,\infty\}$.

The bivectors e_{23}, e_{31} and e_{12} correspond to the Hamilton basis and $E = e_\infty \wedge e_0$ is the Minkowsky plane. The unit Euclidean pseudo-scalar $I_e = e_1 \wedge e_2 \wedge e_3$, the pseudo-scalar $I_c = I_e E$ is used for computing the inverse and duals of multivectors.

Let $x_e = [x, y, z]^T$ be a point expressed in $\mathbb{R}^3$. The representation of this point in the geometric algebra $G_{4,1}$ is given by

$$x_c = x_e + \frac{1}{2} x_e^2 e_\infty + e_0 \tag{1}$$

Given two conformal points x_c and y_c, its difference in Euclidean space can be defined as

$$x_e - y_e = (y_c \wedge x_c) \cdot e_\infty \tag{2}$$

and, consequently, the following equality

$$(x_c \wedge y_c + y_c \wedge z_c) \cdot e_\infty = (x_c \wedge z_c) \cdot e_\infty \tag{3}$$

is fulfilled as well.

The line can be obtained in its standard form as

$$L = nI_e - e_\infty m I_e \tag{4}$$

where n is the orientation and m the moment of the line.

A. Rigid Transformations

These transformations between rigid bodies can be obtained in conformal geometry by carrying out reflections between planes.

A reflection of a point x respect to a plane π is

$$x' = -\pi x \pi^{-1} \tag{5}$$

and for any geometric entity Q is

$$Q' = \pi Q \pi^{-1} \tag{6}$$

The translation can be carrying out by two reflections with parallel planes π_1 and π_2 as

$$Q' = \underbrace{(\pi_2 \pi_1)}_{T_a} Q \underbrace{(\pi_1^{-1} \pi_2^{-1})}_{\tilde{T}_a}, \quad T_a = 1 + \frac{1}{2} a e_\infty = e^{-\frac{a}{2} e_\infty} \tag{7}$$

with $a = 2dn$, d the distance of translation and n the direction of translation.

A rotation is the product of two reflections between nonparallel planes π_1 and π_2 defined by

$$Q' = \underbrace{(\pi_2 \pi_1)}_{R_\theta} Q \underbrace{(\pi_1^{-1} \pi_2^{-1})}_{\tilde{R}_\theta} \tag{8}$$

or computing the conformal product of the normal of the planes n_1 and n_2, yields

$$R_\theta = n_2 n_1 = \cos(\theta/2) - \sin(\theta/2) L = e^{-\theta L/2} \tag{9}$$

with $L = n_1 \wedge n_2$, and θ twice the angle between π_1 and π_2.

The *screw motion* called motor is a composition of a translation and a rotation, both related to an arbitrary axis L. The motor is defined as

$$M = TR\tilde{T} \tag{10}$$

Therefore, a motor transformation for an entity Q is given by

$$Q' = \underbrace{(TR\tilde{T})}_{M_\theta} Q \underbrace{(T\tilde{R}\tilde{T})}_{\tilde{M}_\theta} \tag{11}$$

A more detailed description of Conformal Geometric Algebra can be found in [5] and [6].

III. Dynamic Modeling Using CGA

Based on the equations of kinetic and potential energy and using the Euler-Lagrange formulation, it is possible to synthesize the dynamic model of any n-DOF serial robot manipulator in terms of CGA [7].

The matrix form of the aforementioned equations is given by

$$M(q)\ddot{q} + C(q,\dot{q})\dot{q} + G(q) = \tau \tag{12}$$

Defining m_i, I_j, L'_i and x'_i as the mass, moment of inertia, current axis of rotation and current position of the center of mass for the i^{th} link of the manipulator, respectively, it is possible to re-define equation (12) in the CGA framework using the following matrices

$$M(q) = M_v + M_I \tag{13}$$

where

$$M_I = \delta I = \begin{pmatrix} 1 & 1 & \cdots & 1 \\ 0 & 1 & \cdots & 1 \\ \vdots & \vdots & \ddots & \vdots \\ 0 & 0 & \cdots & 0 \end{pmatrix} \begin{pmatrix} I_1 & 0 & \cdots & 0 \\ I_2 & I_2 & \cdots & 0 \\ \vdots & \vdots & \ddots & \vdots \\ I_n & I_n & \cdots & I_n \end{pmatrix} \tag{14}$$

and

$$M_v = V^T m V \tag{15}$$

with $m = diag\{m_1, m_2, \cdots, m_n\}$ and

$$V = \begin{pmatrix} x'_1 \cdot L'_1 & 0 & \cdots & 0 \\ x'_2 \cdot L'_1 & x'_2 \cdot L'_2 & \cdots & 0 \\ \vdots & \vdots & \ddots & \vdots \\ x'_n \cdot L'_1 & x'_n \cdot L'_2 & \cdots & x'_n \cdot L'_n \end{pmatrix}. \tag{16}$$

Based in the properties of the matrices $M(q), C(q,\dot{q})$ we can define the matrix $C(q,\dot{q})$ as

$$C = V^T m \dot{V} \tag{17}$$

where

$$V = XL = \begin{pmatrix} x'_1 & 0 & \cdots & 0 \\ 0 & x'_2 & \cdots & 0 \\ \vdots & \vdots & \ddots & \vdots \\ 0 & 0 & \cdots & x'_n \end{pmatrix} \begin{pmatrix} L'_1 & 0 & \cdots & 0 \\ L'_1 & L'_2 & \cdots & 0 \\ \vdots & \vdots & \ddots & \vdots \\ L'_1 & L'_2 & \cdots & L'_n \end{pmatrix}. \tag{18}$$

Therefore,

$$\dot{V} = \dot{X}L + X\dot{L} \tag{19}$$

where

$$\dot{X} = \begin{pmatrix} \dot{x}'_1 & 0 & \cdots & 0 \\ 0 & \dot{x}'_2 & \cdots & 0 \\ \vdots & \vdots & \ddots & \vdots \\ 0 & 0 & \cdots & \dot{x}'_n \end{pmatrix} \tag{20}$$

and

$$\dot{L} = \begin{pmatrix} \dot{L}'_1 & 0 & \cdots & 0 \\ \dot{L}'_1 & \dot{L}'_2 & \cdots & 0 \\ \vdots & \vdots & \ddots & \vdots \\ \dot{L}'_1 & \dot{L}'_2 & \cdots & \dot{L}'_n \end{pmatrix}. \tag{21}$$

Finally, the vector $G(q)$ is expressed as the following product

$$G(q) = V^T F \tag{22}$$

with

$$F = \begin{pmatrix} m_1 & 0 & \cdots & 0 \\ 0 & m_2 & \cdots & 0 \\ \vdots & \vdots & \ddots & \vdots \\ 0 & 0 & \cdots & m_n \end{pmatrix} \begin{pmatrix} ge_2 \\ ge_2 \\ ge_2 \\ ge_2 \end{pmatrix} \tag{23}$$

where g is the acceleration due to gravity. For a more detailed explanation of the process to obtain (12) see [7].

IV. Sliding Mode Controller

In this section, the output tracking problem will be developed for the two legs in the biped robot, each with 6-DOF, and a sliding mode controller will be proposed [8].

Due to space limitation the procedure will be explained only for the left leg.

Adding a disturbance term $P(t)$ to (12), we can obtain a state-space representation defining the state variables as $x_1 = q, x_2 = \dot{q}$, the output of the system as $y = x_1$ and the control signal as $U = \tau$. Hence, the resulting state-space model is given by

$$\begin{aligned} \dot{x}_1 &= x_2 \\ \dot{x}_2 &= -M^{-1}(Cx_2 + G) + M^{-1}U + P(t) \end{aligned} \quad (24)$$

the parenthesis were omitted for simplicity. We assume that the disturbance term $P(t)$ is bounded as follows

$$\|P(t)\| < \beta. \quad (25)$$

Defining the output tracking error as

$$e_1 = x_1 - y_{ref}(t). \quad (26)$$

where y_{ref} is the bio-inspired references for the biped robot mentioned in a previous section. Then, the dynamic for e_1 is given by

$$\dot{e}_1 = x_2 - \dot{y}_{ref}(t). \quad (27)$$

Using x_2 as the pseudo-control for this block, we obtain its reference x_{2ref} as

$$x_{2ref} = -k_1 \tanh(\varepsilon_1 e_1) + \dot{y}_{ref}(t). \quad (28)$$

Then, if we define the error variable for the second block as

$$e_2 = x_2 - x_{2ref}. \quad (29)$$

its dynamics can be obtained as

$$\dot{e}_2 = -M^{-1}(Cx_2 + G) + M^{-1}U + P(t) - \dot{x}_{2ref}. \quad (30)$$

The term $\dot{x}_{2ref}$ is defined as

$$\dot{x}_{2ref} = -k_1\varepsilon_1\Phi\left(x_2 - \dot{y}_{ref}(t)\right) + \ddot{y}_{ref}(t)$$

with $\Phi = diag\left\{1 - \tanh^2(\varepsilon_1 e_{11}), \quad \cdots, \quad 1 - \tanh^2(\varepsilon_1 e_{1n})\right\}$

and $e_1 = \begin{bmatrix} e_{11} & \cdots & e_{1n} \end{bmatrix}^T$.

Finally, we design the control law U as

$$U = Cx_2 + G - k_2 M sign(\varepsilon_2 e_2) + M\dot{x}_{2ref}. \quad (31)$$

By means of (31), (30), (28), and (27) the closed loop dynamics for the error variables is given by

$$\begin{aligned} \dot{e}_1 &= -k_1 \tanh(\varepsilon_1 e_1) \\ \dot{e}_2 &= -k_2 sign(\varepsilon_2 e_2) + P(t) \end{aligned} \quad (32)$$

If the conditions $k_1 > 0, k_2 > \beta$ are fulfilled, then the system (32) is globally asymptotically stable [8].

A scheme of our case of study is depicted in figure 1. It is a 3-D virtual representation of the MEXONE humanoid robot from CINVESTAV, Unidad Guadalajara. Each leg of the biped robot has 6 DOF: 3 in the hip, 1 in the knee, and 2 in the ankle.

A. Exact Robust Differentiator

In order to implement the control law defined in (31) we need to know the derivatives $\dot{y}_{ref}(t), \ddot{y}_{ref}(t)$. Obviously, these are unknown terms given that the reference vector $y_{ref}(t)$ was obtained from direct measuring from a walking person.

This lacking information can be achieved by means of a robust differentiator based on high order sliding modes [9]. The structure of a 5^{th}-order differentiator is defined as follows

$$\begin{aligned} &\dot{z}_0 = v_0, \quad v_0 = -12\left|z_0 - y_{ref}(t)\right|^{5/6} sign\left(z_0 - y_{ref}(t)\right) + z_1 \\ &\dot{z}_1 = v_1, \quad v_1 = -8\left|z_1 - v_0\right|^{4/5} sign(z_1 - v_0) + z_2 \\ &\dot{z}_2 = v_2, \quad v_2 = -5\left|z_2 - v_1\right|^{3/4} sign(z_2 - v_1) + z_3 \\ &\dot{z}_3 = v_3, \quad v_3 = -3\left|z_3 - v_2\right|^{2/3} sign(z_3 - v_2) + z_4 \\ &\dot{z}_4 = v_4, \quad v_4 = -1.5\left|z_4 - v_3\right|^{1/2} sign(z_4 - v_3) + z_5 \\ &\dot{z}_5 = -1.1 sign(z_5 - v_4) \end{aligned} \quad (33)$$

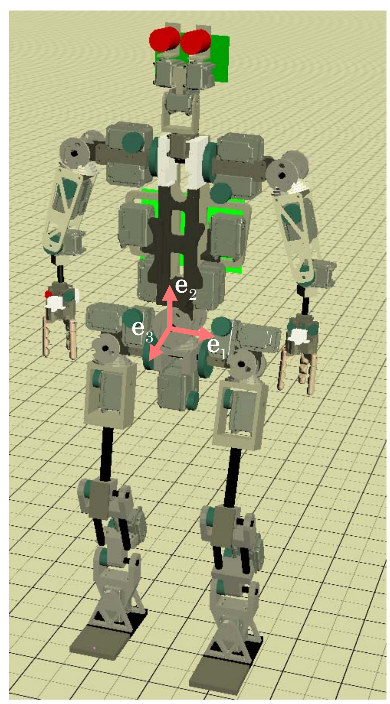

Figure 1. Biped robot with 6-DOF per leg.

where z_i is the estimated i^{th} derivative of y_{ref}, and whose initial value is zero.

Figure 2 shows the bio-inspired walking references for the 6 joints of the left leg and the output of the robust exact differentiator for the first and second derivatives.

V. Simulations

The proposed control law defined in (31) was applied to the biped robot depicted in figure 1. The axes of rotation are defined in figure 2.

The initial value of vector q for the both legs is

$$q = \begin{bmatrix} 0.05 & 0.21 & 0.08 & 0.62 & 0.15 & 0.00003 \end{bmatrix}^T,$$

The gains k_1, k_2 were set as $k_1 = 10 \cdot \begin{bmatrix} 1 & 4 & 1 & 4 & 4 & 2 \end{bmatrix}^T$ and $k_2 = 10 \cdot \begin{bmatrix} 1 & 28 & 1 & 28 & 14 & 4 \end{bmatrix}^T$, respectively. The slopes $\varepsilon_1, \varepsilon_2$ were defined as $\varepsilon_1 = 2, \varepsilon_2 = 5$.

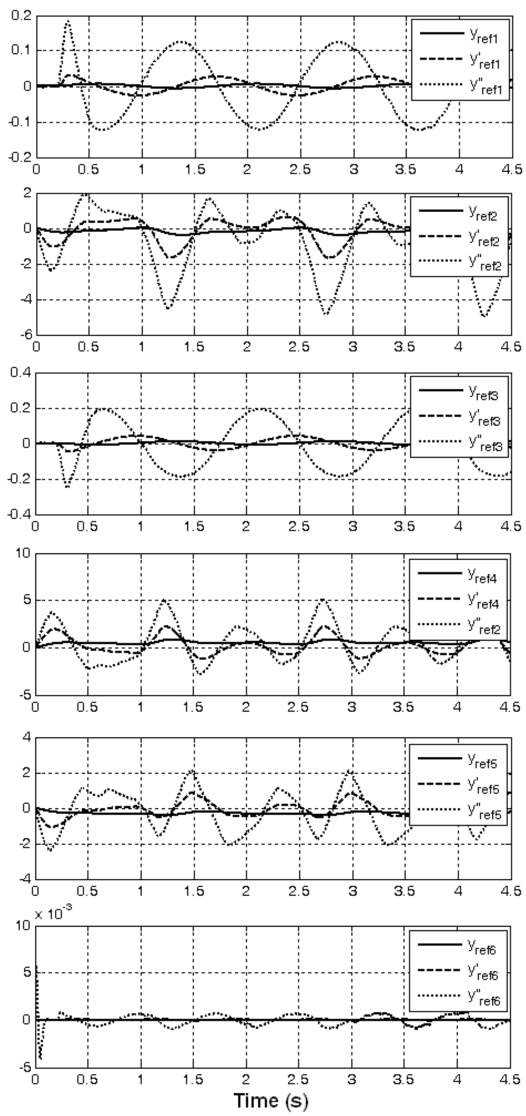

Figure 2. Reference signal, first derivative, and second derivative for the six joints of each leg.

The initial position for the center of mass of each link are

$$\begin{aligned} x_1 &= \sigma_1 e_1 - \sigma_2 e_2 & x_7 &= -\sigma_1 e_1 - \sigma_2 e_2 \\ x_2 &= \sigma_3 e_1 - \sigma_2 e_2 & x_8 &= -\sigma_3 e_1 - \sigma_2 e_2 \\ x_3 &= \sigma_4 e_1 - \sigma_5 e_2 & x_9 &= -\sigma_4 e_1 - \sigma_5 e_2 \\ x_4 &= \sigma_4 e_1 - \sigma_6 e_2 & x_{10} &= -\sigma_4 e_1 - \sigma_6 e_2 \\ x_5 &= \sigma_4 e_1 - \sigma_7 e_2 & x_{11} &= -\sigma_4 e_1 - \sigma_7 e_2 \\ x_6 &= \sigma_4 e_1 - \sigma_8 e_2 & x_{12} &= -\sigma_4 e_1 - \sigma_8 e_2 \end{aligned}$$

and the origins of the frames attached to each link of the biped robot are the following Euclidean points

$$\begin{aligned} o_1 &= \sigma_9 e_1 - \sigma_2 e_2 & o_7 &= -\sigma_9 e_1 - \sigma_2 e_2 \\ o_2 &= \sigma_4 e_1 - \sigma_2 e_2 & o_8 &= -\sigma_4 e_1 - \sigma_2 e_2 \\ o_3 &= \sigma_4 e_1 - \sigma_3 e_2 & o_9 &= -\sigma_4 e_1 - \sigma_3 e_2 \\ o_4 &= \sigma_4 e_1 - \sigma_{10} e_2 & o_{10} &= -\sigma_4 e_1 - \sigma_{10} e_2 \\ o_5 &= \sigma_4 e_1 - \sigma_8 e_2 = o_6 & o_{11} &= -\sigma_4 e_1 - \sigma_8 e_2 = o_{12} \end{aligned}$$

with $\sigma_1 = 0.024, \sigma_2 = 0.062, \sigma_3 = 0.079, \sigma_4 = 0.110,$ $\sigma_5 = 0.068, \sigma_6 = 0.188, \sigma_7 = 0.417, \sigma_8 = 0.533, \sigma_9 = 0.049$ and $\sigma_{10} = 0.302$.

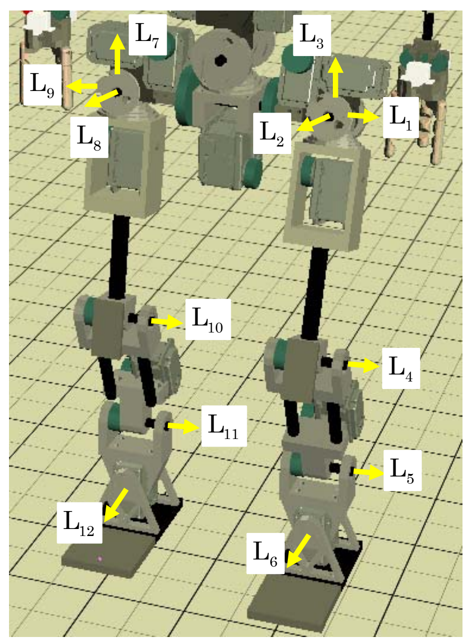

Figure 3. Axes of rotation of the biped robot.

The initial values for the axes of rotation of the biped robot are defined as

$$\begin{aligned} L_1 &= e_{23} + e_\infty (o_1 \cdot e_{23}) & L_7 &= e_{23} + e_\infty (o_7 \cdot e_{23}) \\ L_2 &= e_{12} + e_\infty (o_2 \cdot e_{12}) & L_8 &= e_{12} + e_\infty (o_8 \cdot e_{12}) \\ L_3 &= e_{31} + e_\infty (o_3 \cdot e_{31}) & L_9 &= e_{31} + e_\infty (o_9 \cdot e_{31}) \\ L_4 &= e_{23} + e_\infty (o_4 \cdot e_{23}) & L_{10} &= e_{23} + e_\infty (o_{10} \cdot e_{23}) \\ L_5 &= e_{23} + e_\infty (o_5 \cdot e_{23}) & L_{11} &= e_{23} + e_\infty (o_{11} \cdot e_{23}) \\ L_6 &= e_{12} + e_\infty (o_6 \cdot e_{12}) & L_{12} &= e_{12} + e_\infty (o_{12} \cdot e_{12}) \end{aligned}$$

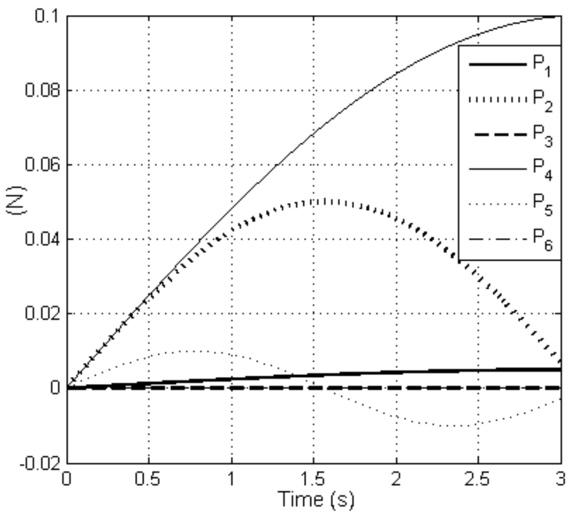

Figure 4. Disturbances used in simulation for each joint of left leg.

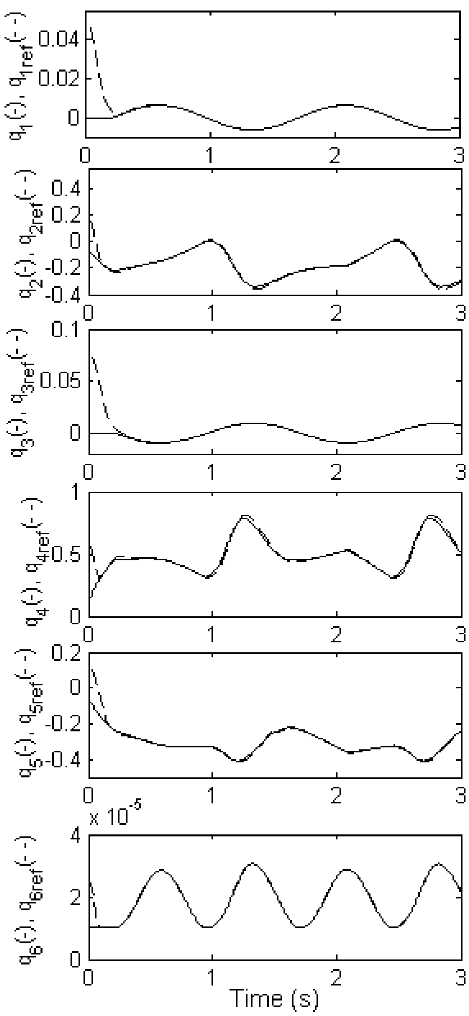

Figure 5. Tracking response for the 6 joints of the left leg.

Due to space limitation, only the simulation results for the left leg will be shown. The performance and response for the right leg are very similar to the left leg. The disturbance signals used in simulation can be appreciated in figure 4. The tracking responses for the 6 joints of the left leg are depicted in figure 5. It can be observed that the control objective is fulfilled and with a low settling time.

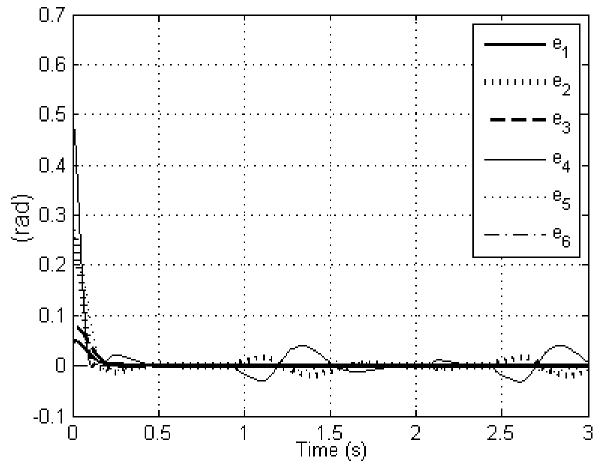

Figure 6. Error variables.

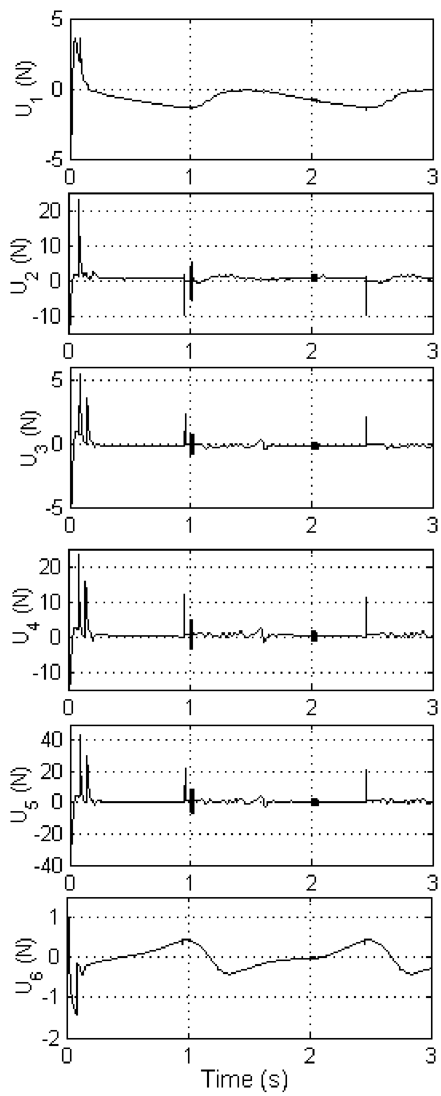

Figure 7. Control signals (joint torques) for the six joints of the left leg

Figure 6 shows that the six corresponding error variables converge to a small vicinity of zero, demonstrating the robustness of the proposed control scheme.

In figure 7, the control signals (torques) of the joints of the left leg are depicted. Finally, a sequence of images of the biped robot walking is presented in figure 8.

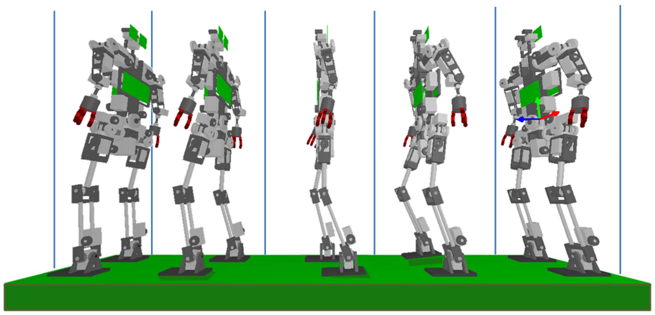

Figure 8. Sequence of images of the biped robot walking.

VI. CONCLUSIONS

The authors apply bio-inspired signals as walking waves to help the manoeuvring of a humanoid robot.

The advantage of using such signal is that they help us to accomplish an expected human like walking of the robot. However this is jeopardized due to the effect of perturbations and non-modelled parameters of the robot dynamics.

To follow such trajectories is necessary to resort to a robust control technique. In addition the algebraic complexity of the formulation is also an issue, which is tackled by computing the kinematics and dynamics of the plant in the conformal geometric algebra framework. As a result, the equations are simple, compact and comfortable to design algorithms subject to geometric constraints. In this regard, the use of a robust sliding mode controller becomes easy and natural.

We present simulations subject to perturbations (pushing, shocking, etc) which confirm the robustness of our control scheme. Future work consists of using more advanced control techniques and real time implementation.

REFERENCES

[1] E. Bayro-Corrochano, *Geometric Computing for Wavelet Transforms, Robot Vision, Learning, Control and Action*, Springer-Verlag, London, 2010.

[2] http://www.pupin.rs/RnDProfile/robotics/hrsp.html

[3] http://www.pupin.rs/RnDProfile/rodic-pub.html

[4] V. Utkin, J. Guldner, and J. Shi, *Sliding Mode Control in Electromechanical Systems*. Ed. Taylor and Francis, 1999, UK.

[5] H. Li, D. Hestenes, and A. Rockwood. "Generalized Homogeneous coordinates for computational geometry". G. Somer, editor, *Geometric Computing with Clifford Algebras*, pp. 27-52. Springer-Verlag, Heidelberg. 2001.

[6] J. Zamora and E. Bayro, "Kinematics and Differential Kinematics of Binocular Heads", in *Proceedings of the International Conference of Robotics and Automation (ICRA'06)*, Orlando, Florida, USA, 2006, pp. 4130-4135.

[7] J. Zamora and E. Bayro-Corrochano, "Parallel Forward Dynamics: a geometric approach", *IROS 2010*, Taiwan, 2010.

[8] L. González-Jiménez, A. Loukianov and E. Bayro-Corrochano, "Integral Nested Sliding Mode Control for Robotic Manipulators", *Proceedings of the 17th World Congress The International Federation of Automatic Control*, Seoul, Korea, pp. 9899 – 9904, 2008.

[9] A. Levant, "Higher Order Sliding Modes, Differentiation and Output Feedback Control", International Journal of Control, Vol. 76, Taylor & Francis, pp. 924-941, 2003.